Evaluation of four-dimensional nonbinary LDPC-coded modulation for next-generation long-haul optical transport networks

Yequn Zhang,* Murat Arabaci, and Ivan B. Djordjevic

Department of Electrical and Computer Engineering, University of Arizona, 1230 E. Speedway Blvd., Tucson, Arizona 85721, USA

yequnz@email.arizona.edu

Abstract: Leveraging the advanced coherent optical communication technologies, this paper explores the feasibility of using four-dimensional (4D) nonbinary LDPC-coded modulation (4D-NB-LDPC-CM) schemes for long-haul transmission in future optical transport networks. In contrast to our previous works on 4D-NB-LDPC-CM which considered amplified spontaneous emission (ASE) noise as the dominant impairment, this paper undertakes transmission in a more realistic optical fiber transmission environment, taking into account impairments due to dispersion effects, nonlinear phase noise, Kerr nonlinearities, and stimulated Raman scattering in addition to ASE noise. We first reveal the advantages of using 4D modulation formats in LDPC-coded modulation instead of conventional two-dimensional (2D) modulation formats used with polarization-division multiplexing (PDM). Then we demonstrate that 4D LDPC-coded modulation schemes with nonbinary LDPC component codes significantly outperform not only their conventional PDM-2D counterparts but also the corresponding 4D bit-interleaved LDPC-coded modulation (4D-BI-LDPC-CM) schemes, which employ binary LDPC codes as component codes. We also show that the transmission reach improvement offered by the 4D-NB-LDPC-CM over 4D-BI-LDPC-CM increases as the underlying constellation size and hence the spectral efficiency of transmission increases. Our results suggest that 4D-NB-LDPC-CM can be an excellent candidate for long-haul transmission in next-generation optical networks.

OCIS codes: (060.0060) Fiber optics and optical communications; (060.4080) Modulation.

References and links

1. Y. Miyamoto and S. Suzuki, "Advanced optical modulation and multiplexing technologies for high-capacity OTN based on 100 Gb/s channel and beyond," IEEE Commun. Mag. **48**(3), S65–S72 (2010).
2. L.-S. Yan, X. Liu, and W. Shieh, "Toward the Shannon limit of spectral efficiency," IEEE Photon. J. **3**, 325–328 (2011).
3. H. G. Batshon, I. B. Djordjevic, and T. Schmidt, "Ultra high speed optical transmission using subcarrier-multiplexed four-dimensional LDPC-coded modulation," Opt. Express **18**(19), 20546–20551 (2010).
4. E. Agrell and M. Karlsson, "Power-efficient modulation formats in coherent transmission systems," J. Lightwave Technol. **27**(22), 5115–5126 (2009).
5. M. Arabaci, I. B. Djordjevic, L. Xu, and T. Wang, "Four-dimensional nonbinary LDPC-coded modulation schemes for ultra high-speed optical fiber communication," IEEE Photon. Technol. Lett. **23**(18), 1280–1282 (2011).
6. I. B. Djordjevic, M. Cvijetic, L. Xu, and T. Wang, "Proposal for beyond 100 Gb/s optical transmission based on bit-interleaved LDPC-coded modulation," IEEE Photon. Technol. Lett. **19**(12), 874–876 (2007).
7. M. Arabaci, I. B. Djordjevic, R. Saunders, and R. M. Marcoccia, "Non-binary quasi-cyclic LDPC based coded modulation for beyond 100 Gb/s transmission," IEEE Photon. Technol. Lett. **22**(6), 434–436 (2010).
8. I. B. Djordjevic, M. Arabaci, and L. L. Minkov, "Next generation FEC for high-capacity communication in optical transport networks," J. Lightwave Technol. **27**(16), 3518–3530 (2009).
9. M. Arabaci, I. B. Djordjevic, R. Saunders, and R. M. Marcoccia, "Polarization-multiplexed rate-adaptive non-binary-quasi-cyclic-LDPC-coded multilevel modulation with coherent detection for optical transport networks," Opt. Express **18**(3), 1820–1832 (2010).

#162963 - $15.00 USD Received 14 Feb 2012; revised 30 Mar 2012; accepted 1 Apr 2012; published 6 Apr 2012

10. M. Tüchler, R. Koetter, and A. Singer, "Turbo equalization: Principles and new results," IEEE Trans. Commun. **50**(5), 754–767 (2002).
11. I. B. Djordjevic, L. L. Minkov, L. Xu, and T. Wang, "Suppression of fiber nonlinearities and PMD in coded-modulation schemes with coherent detection by using turbo equalization," J. Opt. Commun. Netw. **1**(6), 555–564 (2009).

1. Introduction

Growing data-centric services and multimedia-rich internet applications continue to demand further capacity improvements from optical communication networks. The carriers' response to this demand by upgrading their networks to 40 Gb/s dense wavelength-division multiplexing (DWDM) based systems is now outdated and 100 Gb/s deployment has already been started. For future generations of Ethernet operating at even higher data rates, the use of spectrally-efficient multilevel modulation formats is seen as one of the key approaches [1,2]. However, increasing spectral efficiency suggests using larger constellations which in turn degrades resiliency to fiber impairments, i.e., fiber nonlinearities and dispersion effects. Hence, it is of utmost importance to exploit available degrees of freedom meticulously before increasing the order of the modulation format. In this paper, in light of the promising works in the literature [3–5], we distribute the points of a signal constellation over four-dimensional (4D) space rather than constraining them to the conventional 2D space. As we demonstrate, this approach yields longer transmission reaches compared to the corresponding conventional schemes. Aside from the modulation format, the selection of the forward error correction (FEC) scheme is another essential element for long-haul transmission. We employ low-density parity-check (LDPC) codes for FEC since LDPC-coded modulation has been shown to be an excellent candidate for high-speed optical fiber transmission [6,7]. In fact, LDPC-coded modulation with 4D modulation formats has already been studied, as well [3,5]. However, previous works rely on the assumption of amplified spontaneous emission (ASE) noise dominated transmission scenario, and 4D LDPC-coded modulation has not been tested on a realistic optical fiber transmission environment yet. The latter is what this paper is geared toward.

The rest of the paper is organized as follows. Section 2 explicates our optical transmission setup. In Section 3, we describe the transmitter and receiver configurations of the 4D nonbinary LDPC-coded modulation (4D-NB-LDPC-CM) and the prior-art 4D bit-interleaved LDPC-coded modulation (4D-BI-LDPC-CM) schemes. Similarities and differences between the two schemes are also highlighted. Section 4 presents our numerical results. It is shown that the 4D schemes significantly outperform their 2D counterparts employing polarization-division multiplexing (PDM). Furthermore, among the two 4D schemes, 4D-NB-LDPC-CM is shown to be superior to 4D-BI-LDPC-CM. Finally, Section 5 concludes our paper.

2. Optical transmission setup

Our 4D LDPC-coded modulation optical transmission system is depicted in Fig. 1 and is evaluated using VPI Transmission Maker v8.5. Our fiber model takes into account dispersion effects, ASE noise, and impairments due to nonlinear phase noise, Kerr nonlinearities and stimulated Raman scattering. Fiber parameters are listed in Table 1. Our goal is to explore the fundamental limits on the transmission distances that could be achieved by the proposed 4D LDPC-coded modulation schemes (both binary and nonbinary) and compare them against those achievable by its counterpart polarization-division multiplexing 2D LDPC-coded modulation schemes. Thus, we assume perfect chromatic dispersion (CD) and polarization-mode dispersion (PMD) compensation. To achieve this in our simulations, we perform inline CD compensation via dispersion compensating fibers (DCFs) and adopt polarization tracking.

As shown in Fig. 1, each span in the dispersion map consists of a 40km-long single mode fiber (SMF) and a 7.11km-long DCF each followed by an Erbium-doped fiber amplifier (EDFA). We also applied pre-compensation of −320 ps/nm and the corresponding post-compensation in our transmission link. The optimal launch power of the system is found to be near −5 dBm. Bandwidths of the optical and electrical filters are set to $3R_s$ and $0.75R_s$,

#162963 - $15.00 USD Received 14 Feb 2012; revised 30 Mar 2012; accepted 1 Apr 2012; published 6 Apr 2012

respectively, where R_s is the symbol rate which is defined as the information bit rate R_i = 40 Gb/s divided by the FEC code rate R, which is set to R = 0.8, corresponding to 25% (= 1/R - 1) overhead. For efficient encoding and hardware-friendly decoding, we employ regular and quasi-cyclic (QC-) LDPC codes. More specifically, our binary QC-LDPC component code is the (3,15)-regular QC-LDPC(16935, 13550) code whose construction was described in detail in our previous work [8]. The parity-check matrices of the q-ary LDPC codes were obtained by randomly assigning nonzero elements from the finite field of q elements to the 1s in that of the QC-LDPC(16935, 13550) binary code, while ensuring that the QC property is preserved. For more details on how q-ary QC-LDPC codes can be obtained from binary QC-LDPC codes, we refer the interested readers to our previous works [8,9]. In 4D LDPC-coded modulation schemes, we use 16-, 32- and 64-point signal constellations [3]. Our 16-point 4D constellation is described by the set { ± 1, ± 1, ± 1, ± 1}. The 32-4D constellation contains 16 points mapped to different combinations of vectors { ± 0.5, ± 0.5, ± 0.5, ± 0.5}, 4 points mapped to that of { ± 1,0,0, ± 1}, 4 mapped points to that of {0, ± 1, ± 1,0} and 8 points mapped to the different combinations of { ± 1,0,0,0} and its permutations. The coherent receiver is composed of an optical filter, two π-hybrids, eight photodiodes, four electrical filters and four samplers followed by a BCJR-equalizer and LDPC decoder(s).

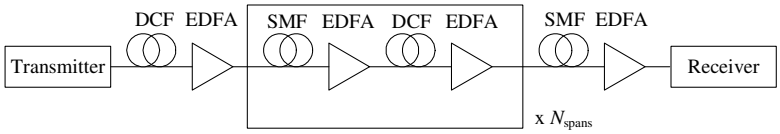

Fig. 1. Dispersion map of the 4D-LDPC-CM transmission system under test.

Table 1. SMF and DCF Parameters

	Length (km)	Attenuation (dB/km)	Dispersion (ps/nm·km)	Dispersion slope (ps/nm^2·km)	Effective cross-sectional area (μm^2)	PMD Coefficient (s/km $^{1/2}$)	Nonlinear refractive index (m^2/W)
SMF	40	0.22	16	0.08	80	0.1×10^{-12}	2.6×10^{-20}
DCF	7.11	0.5	–90	–0.45	30	0.1×10^{-12}	2.6×10^{-20}

3. Four-dimensional nonbinary LDPC-coded modulation

In this section, we describe the transmitter (Tx) and receiver (Rx) configurations of 4D-NB-LDPC-CM scheme, and compare them against those of the prior-art 4D-BI-LDPC-CM scheme. The Tx/Rx structures of 4D-NB-LDPC-CM are depicted in Fig. 2. The source signal entering the transmitter is indeed composed of m parallel binary information streams of length K bits each (see also Fig. 3). We can consider these m parallel bit streams as a single nonbinary stream over an alphabet of $q = 2^m$ symbols. This q-ary information stream of length K is encapsulated into a codeword of length N symbols by a q-ary LDPC encoder of code rate $R = K/N$. The mapper maps each q-ary codeword symbol to a q-ary 4D constellation point $\boldsymbol{s} = (I_x, Q_x, I_y, Q_y)$, where I_x and Q_x correspond to the in-phase and quadrature components in x-polarization, while I_y and Q_y correspond to those in y-polarization. The output of the mapper is used to drive the 4D modulator, composed of a distributed feedback (DFB) laser, a polarization beam splitter (PBS), two I/Q modulators and a polarization beam combiner (PBC). At the Rx side, the received optical signal is first split into two polarizations using the PBS and the resulting signals are fed to two balanced coherent detectors. Outputs of the coherent detectors are sampled at the symbol rate to obtain the estimates on the coordinates corresponding to the transmitted symbols and then passed to the equalizer employing Bahl-Cocke-Jelinek-Raviv (BCJR) algorithm [10, and references therein]. Compared to the conventional 2D schemes where each polarization branch is equipped with a separate BCJR equalizer block, the proposed 4D scheme uses a single BCJR equalizer which handles both polarizations simultaneously, and hence, it can compensate for the nonlinear crosstalk between polarizations, whereas the conventional 2D schemes lack such capability. The BCJR

#162963 - $15.00 USD Received 14 Feb 2012; revised 30 Mar 2012; accepted 1 Apr 2012; published 6 Apr 2012

equalizer is initialized by the probability distribution functions estimated with the help of histograms. The symbol LLRs at the output of the BCJR equalizer are finally forwarded to a q-ary LDPC decoder matched to the encoder at the transmitter side. The estimates of the m information sequences sent by the transmitter are then passed to the sink.

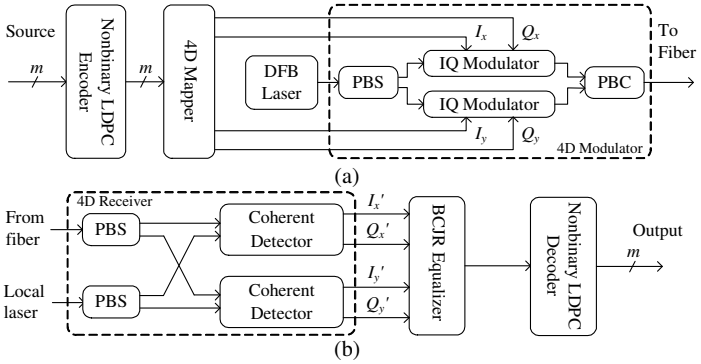

Fig. 2. (a) Transmitter and (b) receiver configurations of 4D-NB-LDPC-CM.

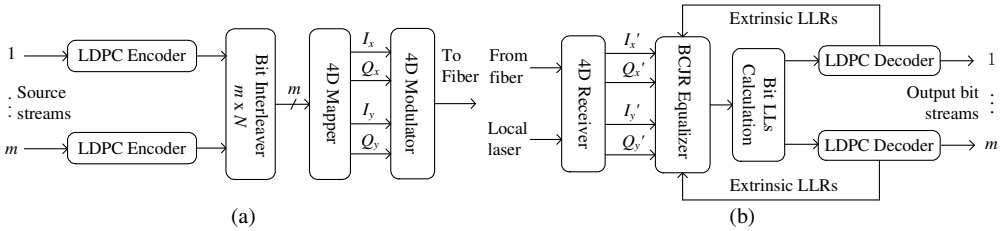

Fig. 3. (a) Transmitter and (b) receiver configurations of 4D-BI-LDPC-CM.

For comparison, we depicted 4D-BI-LDPC-CM Tx/Rx architectures in Fig. 3. The architectures in Fig. 2 and Fig. 3, although look quite similar, bear significant differences. Instead of a single q-ary LDPC encoder, the Tx of 4D-BI-LDPC-CM features m parallel binary LDPC encoders each processing its corresponding information bit stream. To make a fair comparison between the two schemes, in 4D-BI-LDPC-CM, we also consider LDPC codes with code rates $R = K/N$ in each parallel branch. The codewords are then placed in an $m \times N$ block-interleaver row-wise. The mapper reads the data out of the interleaver column-wise and maps the m-bit tuple to a 2^m-ary constellation symbol. The rest of the operations are the same as those performed by the Tx of 4D-NB-LDPC-CM. At the Rx side, as the binary LDPC decoders require bit LLRs to initialize the decoding process, the symbol LLRs produced by the BCJR equalizer are converted to bit LLRs. Upon decoding, the extrinsic information (bit LLRs after decoding minus those before decoding) from the LDPC decoders are fed back to the BCJR equalizer. This is the infamous turbo equalization operation [6,10,11]. (Note that although omitted in Fig. 3, the bit LLRs are combined to form symbol LLRs which are used by the BCJR equalizer as the a priori estimates on symbol LLRs). The underlying idea behind turbo equalization is to exploit the inherent dependence between bits of a transmitted symbol by combining the reliability estimates obtained by independently operating binary LDPC decoders on the bits of a transmitted symbol to form an initial reliability estimate on the transmitted symbol itself. In fact, such a feedback mechanism is of critical importance for bit-interleaved LDPC-coded modulation [6,10,11]. The turbo-like decoder will stop when either convergence is achieved or a predefined number of feedback iterations is reached. In 4D-BI-LDPC-CM, we perform the maximum of 25 iterations in each binary LDPC decoder, and perform 3 outer iterations between the binary LDPC decoders and the BCJR equalizer. Thus, binary LDPC decoders are allowed to run for a maximum of 100 (= 25 x 4) iterations in total. In 4D-NB-LDPC-CM, on the other hand, there is no need for outer iteration since both the

#162963 - $15.00 USD Received 14 Feb 2012; revised 30 Mar 2012; accepted 1 Apr 2012; published 6 Apr 2012

equalizer and the nonbinary decoder operate on the q-ary state space. In order to provide 4D-NB-LDPC-CM with a comparable number of iterations, we set the number of decoding iterations in q-ary LDPC decoder to the maximum of 50 iterations. Although this gives an advantage to the BI-LDPC-CM in terms of the total number of decoding iterations, we observed that running more than 50 iterations in nonbinary LDPC decoders does not enhance error correction performance.

4. Numerical results and analysis

In order to attest the advantages of using 4D modulation formats, 4D LDPC-coded modulation schemes (both binary and nonbinary) are compared to their conventional counterparts employing PDM and 2D signal constellations, whose Tx and Rx configurations can be found in [6] for binary and in [7] for nonbinary LDPC-coded modulation. Effectively, 4D schemes use the state of polarization to define a larger signal constellation whereas PDM-2D schemes use it for multiplexing. For a fair comparison between the two schemes, we need to compare them when they both attain the same information bit rate. Regardless of being binary or nonbinary LDPC-coded modulation, if we assume that both the 4D scheme and the corresponding PDM-2D scheme operate at the same symbol rate of R_s symbols/s and that they both employ component LDPC codes of code rate R, the information bit rate of the 4D scheme is given by $RR_s\log_2(M_{4D})$ and that of the PDM-2D scheme is given by $2RR_s\log_2(M_{2D})$, both in information-bits/s, where M_{4D} and M_{2D} are the constellation sizes used in the 4D scheme and the PDM-2D scheme, respectively. Thus, the proposed 4D scheme is comparable to a PDM-2D scheme, in aggregate data rate, when $M_{4D} = (M_{2D})^2$. For example, the 4D scheme with a signal constellation of size 16, which will be called as the 16-4D scheme, is comparable to PDM-QPSK. Similarly, 64-4D scheme is comparable to PDM-8QAM. The aggregate bit rates then become (i) $4 \times 50 \times 0.8 = 160$ Gb/s for 16-4D and PDM-QPSK, and (ii) $6 \times 50 \times 0.8 = 240$ Gb/s for 64-4D and PDM-8QAM.

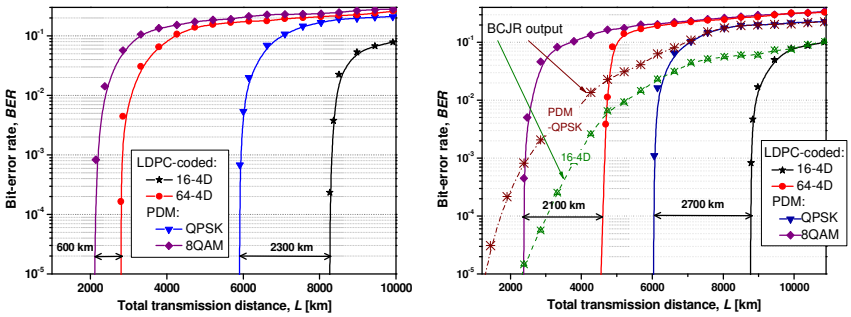

Fig. 4. BER vs. transmission distance comparisons between (a) 4D-BI-LDPC-CM and PDM-2D-BI-LDPC-CM, and (b) 4D-NB-LDPC-CM and PDM-2D-NB-LDPC-CM.

In Fig. 4(a), we present first the bit error rate (BER) against transmission distance performances of 4D-BI-LDPC-CM and the corresponding PDM-2D bit-interleaved LDPC-coded modulation (PDM-2D-BI-LDPC-CM) schemes under the dispersion map given in Fig. 1. Our comparisons are based on the modulation formats mentioned in the previous paragraph, i.e., 16-4D versus PDM-QPSK and 64-4D versus PDM-8QAM. As shown in Fig. 4(a), we achieve more than 8000 km with 16-4D at 160 Gb/s aggregate bit rate and 2800 km with 64-4D at 240 Gb/s aggregate bit rate. The corresponding PDM-QPSK and 8QAM distances are limited to around 6000 km and 2000 km, respectively. We observe a similar trend in our comparison between 4D-NB-LDPC-CM and PDM-2D nonbinary LDPC-coded modulation (PDM-2D-NB-LDPC-CM) whose results are presented in Fig. 4(b). As the two figures reveal, while 4D scheme loses its appeal over the corresponding PDM-2D scheme when binary LDPC-coded modulation is used (i.e., the additional transmission distance provided by 4D scheme gets significantly smaller), there is a solid advantage in using a 4D

#162963 - $15.00 USD Received 14 Feb 2012; revised 30 Mar 2012; accepted 1 Apr 2012; published 6 Apr 2012

scheme over the corresponding PDM-2D scheme even with large constellation sizes if nonbinary LDPC-coded modulation is used. To put it numerically, 4D-NB-LDPC-CM maintains more than 2000 km additional transmission reach over PDM-2D-NB-LDPC-CM during transmission at aggregate bit rates of both 160 Gb/s and 240 Gb/s. Such an improvement in transmission reach is just a well-grounded justification why 4D schemes should be adopted rather than PDM-2D schemes for long-haul transmission. We also present the BER performance of the BCJR equalizer output in Fig. 4(b) to illustrate the capability of nonlinear polarization crosstalk compensation of 4D LPDC-coded modulation.

In order to further manifest the superiority of 4D-NB-LDPC-CM over 4D-BI-LDPC-CM, we performed comparisons between the two for three different 4D modulation formats, i.e., 16-, 32- and 64-4D. Our results are presented in Fig. 5. Note that, in addition to 16-4D and 64-4D constellations, we also included simulations with 32-4D constellation into Fig. 5 in order to obtain a better insight into how the performances of 4D-BI-LDPC-CM and 4D-NB-LDPC-CM change as the underlying 4D constellation size changes. Concurring with the results obtained under ASE noise dominated transmission scenario presented in [7], 4D-NB-LDPC-CM significantly outperforms 4D-BI-LDPC-CM especially as the underlying constellation size, and hence the spectral efficiency, and hence the aggregate bit rates increase. For example, for transmission at 240 Gb/s, 4D-NB-LDPC-CM can provide more than 1500 km additional reach compared to 4D-BI-LDPC-CM. In addition to improving transmission reach compared to 4D-BI-LDPC-CM, 4D-NB-LDPC-CM can also improve the latency at the receiving ends since it avoids costly turbo equalization steps which passes through the inherently complex BCJR equalization block about 3 to 5 times for acceptable performance in BI-LDPC-CM schemes [3,6,11].

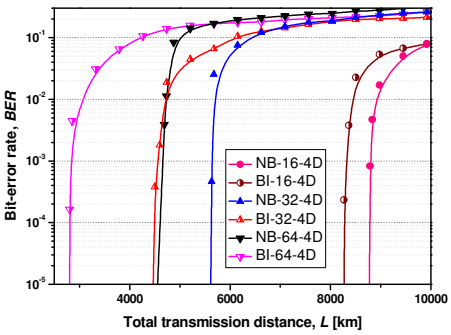

Fig. 5. BER vs. transmission distance comparison of 4D-NB-LDPC-CM and 4D-BI-LDPC-CM.

5. Conclusion

We have evaluated the performance of four-dimensional nonbinary LDPC-coded modulation scheme suitable for next-generation optical transport networks (OTNs). We first revealed the advantages of utilizing a higher-dimensional modulation format in LDPC-coded modulation by comparing 4D schemes with the corresponding PDM-2D schemes. Further, we demonstrated that 4D-NB-LDPC-CM is much more advantageous to use compared to 4D-BI-LDPC-CM as it provides longer transmission reaches. We also noted than the improvement in transmission reach offered by 4D-NB-LDPC-CM over 4D-BI-LDPC-CM increases with increasing constellation size and hence increasing spectral efficiency, which is the direction that optical fiber communication is going toward. Given their superior performances, we strongly advocate adopting 4D-NB-LDPC-CM schemes over both 4D-BI-LDPC-CM and PDM-2D schemes for next-generation OTNs.

Acknowledgments

This work was supported in part by NSF under Grant CCF-0952711.

#162963 - $15.00 USD Received 14 Feb 2012; revised 30 Mar 2012; accepted 1 Apr 2012; published 6 Apr 2012